ARR No. L6A16

Copy 1

NATIONAL ADVISORY COMMITTEE FOR AERONAUTICS

WARTIME REPORT

ORIGINALLY ISSUED

March 1946 as
Advance Restricted Report L6A16

EFFECT OF ROTOR-TIP SPEED ON HELICOPTER HOVERING PERFORMANCE AND MAXIMUM FORWARD SPEED

By F. B. Gustafson and Alfred Gessow

Langley Memorial Aeronautical Laboratory
Langley Field, Va.

NACA

WASHINGTON

NACA ARR No. L6A16

NATIONAL ADVISORY COMMITTEE FOR AERONAUTICS

ADVANCE RESTRICTED REPORT

EFFECT OF ROTOR-TIP SPEED ON HELICOPTER HOVERING PERFORMANCE AND MAXIMUM FORWARD SPEED

By F. B. Gustafson and Alfred Gessow

SUMMARY

A specific study was made of several sample helicopters in order to evaluate the effect of rotor-tip speed on hovering performance and limiting forward speed. The purpose of this study was to determine whether hovering performance could be increased by the use of lower tip speeds without undue sacrifice in maximum forward speed. The types investigated were: (1) a helicopter typical of current conventional design, (2) a similar machine of lower solidity than the first, and (3) a relatively high-powered, cleanly designed "high-speed" helicopter. The effects of blade twist and of blade-section stalling angle of attack on limiting forward speed are discussed. In each case the limiting forward speed was determined as the speed at which the tip of the retreating blade reached the stalling angle. Limiting angles of attack of 12° and 16° were investigated.

A study of the "typical" helicopter indicated that improved hovering performance could be obtained with no loss in maximum speed by the use of lower operating tip speeds at the maximum power output of the engine. This reduction in tip speed and the resulting reduction in limiting forward speed did not cause a corresponding reduction in the maximum forward speed of the helicopter, inasmuch as the operating tip speed before reduction was higher than that necessary to prevent tip stall at the maximum forward speed as fixed by the engine power available. The improvement in hovering performance is relatively small, however, unless advantage is taken of blade twist and of airfoil sections having high stalling

angles. A study of the "low-solidity" helicopter revealed that, although higher rotor-tip speeds than for the typical helicopter are required (for a given limiting forward speed) because of the decrease in solidity, improved hovering performance could be obtained by employing lower tip speeds than are now in use.

For either the typical or the low-solidity helicopter, after the tip speed has been reduced to the point where tip stalling will occur at maximum forward speed, some further improvement in hovering performance may be obtained by using still lower tip speeds. If a single engine-to-rotor gear ratio is used, however, the reduction in maximum forward speed due to tip stall is extremely rapid.

The impossibility of obtaining hovering performance reasonably near the optimum together with relatively high forward speeds with a single gear ratio is illustrated by the "high-speed" helicopter. A gear shift that enables full power to be drawn at low tip speeds in hovering flight and at high tip speeds in maximum-forward-speed flight appears to be mandatory for obtaining both high speeds and near-optimum hovering performance.

INTRODUCTION

Generalized treatments of helicopter rotor theory have long indicated that, for a given disk loading and solidity, the choice of rotor-blade tip speed greatly affects the performance of helicopters in the hovering and forward-flight conditions and that the tip-speed requirements in the two flight conditions are conflicting. Theory has shown that optimum hovering performance is obtained when the blade elements are operating near the stalling angle of attack (fig. 3 of reference 1). This condition results from the fact that, if the chord is fixed but the tip speed can be varied, profile-drag power is a minimum when the blade sections operate at an angle of attack such that the ratio of the cube of the lift coefficient to the square of the profile-drag coefficient is a maximum. It may be concluded from figure 1 that

this condition occurs near the stalling angle for conventional sections. Flight tests have supported the theoretical conclusions in that minimum power for a fixed static thrust was required when the helicopter was operating at the lowest tip speed that was considered safe without the use of an automatic pitch-control mechanism (unpublished data). Although the same angle-of-attack requirement holds true in the forward-flight condition, tip speeds must be relatively higher than those used in hovering in order to avoid stalling the retreating blade and thus prevent the increased vibration, loss of control, and loss of rotor efficiency associated with tip stall.

In order to determine whether an increase in hovering performance of current helicopters could be obtained by reducing the rotor-tip speed without unduly limiting the maximum forward speed, a specific study of the effect of tip speed on the hovering performance and limiting forward speed of several typical designs was believed to be of value. Several designs were studied in order to illustrate the effect of changes in helicopter design parameters on the choice of tip speed for a particular flight condition.

SYMBOLS

W	gross weight of helicopter, pounds
R	radius of main-rotor blades measured from axis of rotation to tip of blades, feet
Ω	angular velocity of main rotor, radians per second
ρ	mass density of air, slugs per cubic foot
T	rotor thrust, pounds
C_T	thrust coefficient $\left(\frac{T}{\rho(\Omega R)^2 \pi R^2}\right)$
Q_o	rotor profile-drag torque, foot-pounds
Q_i	induced rotor torque, foot-pounds

$Q_{P.E.}$ torque required to change the potential energy of the helicopter (climb condition), foot-pounds

Q total torque, foot-pounds $\left(Q_o + Q_i + Q_{P.E.}\right)$

C_{Q_o} profile-drag torque coefficient $\left(\frac{Q_o}{\rho(\Omega R)^2 \pi R^3}\right)$

$\left(C_{Q_i}, C_{Q_{P.E.}}, \text{ and } C_Q \text{ are likewise defined as } Q_i, Q_{P.E.}, \text{ or } Q \text{ divided by } \rho(\Omega R)^2 \pi R^3\right)$

r distance of a rotor-blade element from axis of rotation, feet

$x = \frac{r}{R}$

c_e equivalent chord, feet $\left(\frac{\int_0^R cr^2\,dr}{\int_0^R r^2\,dr}\right)$

c rotor-blade chord at radius r, feet

b number of blades

σ rotor solidity $\left(\frac{bc_e}{\pi R}\right)$

V_v rate of vertical climb, feet per second

v induced inflow velocity parallel to axis of rotation, feet per second

u total flow through rotor disk, feet per second $(V_v + v)$

a_o slope of curve of lift coefficient against section angle of attack (radian measure), assumed to be 5.73

α_o section angle of attack, measured from line of zero lift, radians

$a_{(1.0)(270^\circ)}$	section angle of attack at tip of retreating blade at 270° azimuth angle, radians
c_{d_o}	section profile-drag coefficient
δ_o, δ_1, δ_2	coefficients used in defining the profile-drag curve $c_{d_o} = \delta_o + \delta_1 a_o + \delta_2 a_o^2$
c_l	section lift coefficient
θ	blade-section pitch angle, radians
θ_T	blade-tip pitch angle, radians
ϕ	induced angle of attack, radians $\left(\frac{u}{\Omega r}\right)$
ϕ_T	induced tip angle of attack, radians

SAMPLE DESIGNS STUDIED

The design characteristics of the three helicopters studied are as follows:

Type	Gross weight (lb)	Main-rotor shaft power (hp)	Rotor solidity	Rotor diameter (ft)	Fuselage parasite-drag area (sq ft)
Typical	2700	200	0.060	41	15
Low-solidity	2700	200	.045	41	15
High-speed	3300	300	.060	41	6

Blade plan form: Rectangular

Blade twist: -8° (in forward-flight calculations)

Rectangular blades were used in the calculations because of the ease in calculating the performance characteristics of nontapered blades. The differences in

performance incurred by using a nontapered plan form rather than the more commonly used tapered plan form are not expected to be of sufficient magnitude to affect the general conclusions drawn from this analysis, especially in view of the comparative nature of the calculations presented. The choice of blade twist in the calculations of vertical and forward flight is discussed in the section "Method of Analysis."

The brake horsepower corresponding to the main-rotor shaft power listed can be computed by assuming a gearing, cooling, and tail-rotor loss of 20 percent.

The parameters for the "typical" helicopter were chosen to illustrate a helicopter of current design. The "low-solidity" differs from the typical helicopter only in a 25-percent reduction in solidity and was chosen to illustrate the effect of solidity on the choice of compromise tip speeds. This choice of a single tip speed for a particular design is affected by the amount of power and the cleanness of the fuselage, inasmuch as less increase in tip speed for forward flight is necessary if low power and high parasite drag limit the speed of the helicopter at the start. Thus a "high-speed" helicopter was chosen, the parameters of which represent a design that might be evolved when an appreciable increase in helicopter maximum forward speed is desired. Because of the 50-percent increase in power over that of the typical example, the weight of the helicopter was increased to 3300 pounds (corresponding to a disk loading of 2.5 lb/sq ft) in order to take advantage of the increased available static thrust and to allow for the additional structural and engine weight necessitated by the increased power.

METHOD OF ANALYSIS

Hovering and Vertical-Flight Performance

The performance of the sample helicopters in the hovering and vertical-flight conditions was computed as a function of tip speed by means of the general performance equation derived in the appendix. The development of the equation was based on assumptions similar to those used in deriving the forward-flight performance equations

of references 2 and 3, which are subsequently used to calculate limiting forward speeds. Specifically, the assumptions included:

(1) The inflow is uniform across the rotor disk. In forward flight, uniform inflow is assumed to exist regardless of blade twist. In the hovering condition and at small rates of climb, uniformity of inflow is more significant than in forward flight and can be assumed to be achieved by twisting the blade so that the angle of attack of each element varies inversely as the distance of the element from the center of rotation. This pitch variation is known as the "ideal" twist and has been adopted herein for the study of vertical flight.

(2) The profile characteristics of the blade elements can be represented by a three-term power series. The equation representing the section profile-drag coefficient is therefore expressed as

$$c_{d_o} = \delta_o + \delta_1 \alpha_o + \delta_2 \alpha_o^2 \qquad (1)$$

where α_o is the section angle of attack measured from the line of zero lift and the coefficients δ_o, δ_1, and δ_2 define the shape of the drag curve and the magnitude of the drag coefficient. For the example presented in this report, the variation of profile-drag coefficient with angle of attack used in both the vertical- and forward-flight performance calculations is represented by

$$c_{d_o} = 0.0087 - 0.0216\alpha_o + 0.400\alpha_o^2 \qquad (2)$$

The corresponding profile-drag curve is shown in figure 1 and represents conventional semismooth airfoils (drag of smooth airfoils increased by a roughness factor of 17 percent). This curve yields a minimum profile-drag coefficient of 0.0084 and is representative of well-built plywood blades.

It should be noted that, for a given helicopter, the variation of calculated vertical-flight performance with tip speed is a function of rotor profile drag only and therefore is directly dependent upon the drag curve.

Consequently the choice of operating tip speeds arrived at by calculations comparing vertical and maximum-forward-speed flight, such as are presented in this report, will depend on the drag curve used. In general this choice will become more critical with an increase in magnitude of the values of drag coefficient.

(3) The blade elements beyond 0.97 radius are assumed to produce profile drag but no thrust. In order to be consistent with the assumptions used in the forward-flight analysis, the entire rotor disk was used in calculating induced losses, even though the relative importance of these losses is greater in hovering flight.

Consistent with these assumptions, the general performance equation for the vertical-climb condition is

$$C_Q = \frac{1}{2}\frac{C_T}{0.941}\sqrt{\left(\frac{V_v}{\Omega R}\right)^2 + \frac{2C_T}{0.941}} + \frac{1}{2}\left(\frac{V_v}{\Omega R}\right)\frac{C_T}{0.941} + \frac{\sigma}{8}\delta_o + \frac{2}{3}\frac{\delta_1}{a_o}\frac{C_T}{0.941} + \frac{4\delta_2}{\sigma a_o^2}\left(\frac{C_T}{0.941}\right)^2 \quad (3)$$

The derivation of this equation is given in the appendix.

Equation (3) was used in plotting the vertical-climb performance charts shown in figure 2(a) for a solidity of 0.060 (typical and high-speed cases) and in figure 2(b) for a solidity of 0.045 (low-solidity case). Values of the coefficients δ_o, δ_1, and δ_2 appearing in the profile-drag equation (equation (1)) were obtained from equation (2).

Hovering performance may be calculated by means of the $V_v/\Omega R = 0$ curves in figure 2.

The assumption of ideal twist (or uniform downwash) results in absolute values of hovering performance that are higher than would be predicted for conventionally twisted blades. Consistent errors of this magnitude (3 to 8 percent, depending on the amount of twist

employed), however, will not appreciably affect the usefulness of the comparative calculations presented. It should also be noted that the use of ideal twist calls for a changed blade pitch distribution with different thrust coefficients and rates of climb (see equation (A17) of appendix).

The power required for a helicopter of given weight operating at varying tip speeds and the thrust developed at different tip speeds for a given power were computed for standard sea-level conditions by means of figure 2. The rate of climb for a given available power and a given thrust was also obtained from figure 2 by noting the value of $V_v/\Omega R$ for given values of $2C_Q/\sigma a_o$ and $2C_T/\sigma a_o$.

With the assumptions used, the profile-drag power in the hovering and vertical-flight conditions is identical for a rotor assumed to be twisted so as to produce uniform inflow in each condition, inasmuch as the angle-of-attack distribution is the same in both cases.

Forward-Flight Performance

Aside from power considerations, the maximum forward speed of the sample helicopters was assumed to be limited by the stalling angle of the retreating blade. Although this criterion is not exact, it is in general a good indication of the speed at which excessive vibration, loss of control, and sharply increased power requirements occur. This limiting condition is borne out by pilots' observations in flight insofar as vibration and loss of control are concerned (unpublished data); and theoretical investigations based on graphical analysis indicate that the reduction in rotor efficiency following tip stall is great enough to place a practical limit on the forward speed of the aircraft (reference 1).

At a given rotor-tip speed, disk loading, and solidity, the forward speed at which tip stall occurs is a function

of the blade design. If uniform inflow is assumed, the only significant factors are the blade twist and the airfoil section employed. The effects of twist and airfoil section are illustrated by figure 3, which shows the difference in limiting speed for blades having 0° twist and -8° twist at limiting tip angles of 12° and 16° (measured from the line of zero lift). The calculations were made for an altitude of 5000 feet, which was assumed to be the highest altitude at which top speed would frequently be maintained. The calculations for 0° twist were computed by means of the performance charts presented in reference 3, and those for -8° twist were based on similar unpublished charts. The inboard stalling limits that were used in reference 3 in addition to the tip stalling limits have been ignored in the present treatment. The simplification in the presentation is believed to be justified inasmuch as the tip stalling limits occur prior to the inboard limits at and above the maximum forward speed indicated in each of the examples given. Likewise, no Mach number limits are shown. Calculations for the sample high-speed helicopter give a maximum Mach number of 0.78 for the advancing blade tip and 0.33 for the retreating blade tip at full power when operating at the 12° limiting angle. Present knowledge of compressibility phenomena indicate that these values are not beyond the practical operating range. The highest blade Mach numbers occur at azimuth angles at which the section angles of attack are lowest (advancing blade), whereas the lowest Mach numbers occur at the higher angles of attack (retreating blade). This condition tends to equalize the effects of compressibility around the rotor disk.

Figure 3 shows that at the currently used tip speed of 500 feet per second for full power, -8° twist extends the limiting forward speed by 11 miles per hour when the stalling angles of the tip sections occur at 16° and by 16 miles per hour when the stalling angles occur at 12°. This figure also indicates that the substitution of a section providing an increase in stalling angle from 12° to 16° raises the limiting speed by about 20 miles per hour. In turn, the stalling angle of a section depends on such factors as camber, leading-edge radius, and

thickness of the airfoil section employed. An increase in stalling angle (as measured from the line of zero lift) of several degrees might be achieved, for example, by the substitution of the NACA 23012 airfoil section for the NACA 0012 section.

The importance of twist and proper airfoil section in delaying tip stall and thereby increasing the limiting forward speed is thus apparent. Conversely, if a given limiting speed is chosen, a lower tip speed may be used, with resulting gains in hovering performance. Because twist can thus be used to reduce the necessity for compromise between hovering performance and maximum forward speed when a fixed tip speed (single gear ratio) is used, the sample calculations were made for blades incorporating -8° twist.

RESULTS AND DISCUSSION

Calculations of limiting forward speed and hovering performance for the typical, low-solidity, and high-speed example helicopters are shown in figures 4, 5, and 6, respectively. The ends of the solid parts of the limiting-forward-speed curves in figures 4(a), 5(a), and 6(a) indicate the limits of available power for the sample helicopters. For the typical and low-solidity helicopters, the 200 horsepower available at the main-rotor shaft at sea level is assumed to be reduced to 170 horsepower at an altitude of 5000 feet if an unsupercharged engine is used. For the high-speed example helicopter, the 300 horsepower available at sea level was assumed to be maintained at an altitude of 5000 feet by supercharging.

Typical Helicopter

Figure 4 illustrates the conflicting tip-speed requirements of vertical and forward flight. This figure shows that the loss in maximum forward speed due to a reduction in tip speed is rapid throughout the entire tip-speed range if the maximum forward speed is not limited at any speed by the low available power or by high parasite drag. The combination of low-power limitation and relative flatness of the vertical-flight performance curves in the low-tip-speed range enables a compromise

tip speed to be chosen so that neither vertical-flight performance nor maximum forward speed is greatly curtailed.

For the typical helicopter current practice would place the tip speed corresponding to maximum power at approximately 500 feet per second. Figure 4 shows that improved hovering performance can be obtained by the use of a lower tip speed without any loss of maximum forward speed, provided that blade twist and an airfoil section having a high stalling angle are incorporated. If it were assumed that the rotor-blade tip sections had a stalling angle of 16°, a reduction in tip speed from 500 to 445 feet per second would cause no reduction in maximum forward speed (because of insufficient power to take advantage of higher tip speeds) and the hovering performance would be increased as follows: a decrease of 13 horsepower (8.1 percent) in power required for hovering at fixed weight, or an increase of 150 pounds (4.5 percent) in thrust available at fixed power (200 hp), or an increase of 215 feet per minute (26.7 percent) in rate of vertical climb at fixed weight and power. These changes are more significant when useful load is considered; for example, although an increase in take-off thrust of 150 pounds is only a 4.5-percent increase in total thrust, it represents approximately 25-percent increase in useful load for current helicopters. If the 12° limiting angle were adhered to (present designs operate near this condition at top speed), the maximum forward speed would be reduced by 16 miles per hour, if the same improvement in hovering performance is desired. In this case, the compromise tip speed of 445 feet per second would be strongly in favor of the hovering performance.

Small additional gains in vertical-flight performance could be obtained by using still lower tip speeds such as 400 feet per second, but these gains would be obtained at great expense in limiting forward speed. For example, if the sample helicopter were flying at a limiting tip angle of 16°, a decrease in tip speed from 445 feet per second to 400 feet per second would result in a decrease in maximum forward speed of 22 miles per hour.

Low-Solidity Helicopter

Comparison of figure 5 with figure 4 indicates that if operation at the same limiting angle of attack is

assumed for both solidities, the maximum forward speed at 5000 feet for 170 horsepower and the vertical-flight performance (at the tip speeds corresponding to the maximum forward speeds at the limiting angle of attack) are virtually the same (within 1 percent) for the two solidities compared. The tip speeds for corresponding limiting-forward-speed conditions, however, are of course increased for the helicopter of lower solidity. The improvements in hovering performance that may be made by reducing the tip speed as a result of operating at higher tip angles of attack (for example, by using a limiting angle of attack of 16° as compared with 12°) are found to be practically the same as for the 0.060 solidity. Also, as was true with the higher solidity, small additional gains in vertical-flight performance may be had by operating at tip speeds below those set by adhering to a limiting angle of attack of 16° in forward flight at full power but only at great expense in limiting forward speed as long as a fixed gear ratio is used.

The almost identical performance obtained in both hovering and forward flight for the two solidities, when the tip speeds are adjusted to give the same limiting forward speed, should not be taken as representing a general rule inasmuch as several compensating effects are involved, the relative magnitude of which will change when different values are chosen for the various parameters. For the present example, however, the choice of the combination of tip speed and solidity would depend on other factors, such as required spar depth, relative importance of stresses due to torque and centrifugal force, performance in autorotation, and endurance and maximum rate of climb in forward flight. Further, when the maximum forward speed of helicopters becomes high enough to result in reaching critical Mach numbers at the blade tips, relatively high solidities will be needed in order to reduce the tip speed required by the stalling limits.

High-Speed Helicopter

As the general performance characteristics of the helicopter are improved, the demand for relatively high-speed flight will result in the use of high-powered, cleanly designed machines. Figure 6 shows that if the available power is to be fully utilized in both hovering

and high-forward-speed flight with this type of helicopter, a compromise tip speed will give satisfactory performance at one end of the speed range only at great expense in performance at the other.

If the engine were supercharged to give a critical altitude of 5000 feet or more, the power available for the case considered would be 300 horsepower, which would result in a possible top speed of 166 miles per hour for a limiting stalling angle of 12°. If a tip speed of 606 feet per second, which corresponds to this speed and limiting stalling angle, is used, the hovering performance will be greatly reduced from that available at lower tip speeds. For example, the hovering performance as compared with that for a tip speed of 400 feet per second would be reduced as follows: an increase of 55 horsepower (30 percent) in power required to hover at fixed weight, or a decrease of 490 pounds (10 percent) in thrust available at fixed power (300 hp), or a decrease of 680 feet per minute (39 percent) in rate of vertical climb at fixed weight and power. These increments would be reduced to about two-thirds of the values given if a limiting angle of 16° instead of 12° were chosen. If continuous operation at or near maximum forward speed is desired, it appears possible that the choice of limiting angle may be dictated by considerations of vibration, at least until there are further developments in vibration absorption. When the choice is made on this basis, the limiting angle may be appreciably lower than the stalling angle of the section.

If both high-speed and near-optimum hovering performance are desired, the advantages of a gear shift that enables full engine power to be drawn at two tip speeds becomes apparent. For the case just considered a tip speed of 400 feet per second would be chosen for the hovering condition and 600 feet per second for the high-speed flight condition; thus the loss in vertical-flight performance indicated in the previous paragraph would be avoided and the limiting forward speed would not be lowered.

CONCLUSIONS

The calculations of vertical-flight performance and limiting forward speed (as set by tip stall) made for

three sample helicopter designs indicate the following conclusions:

1. The hovering performance of helicopters typical of current design can be improved without unduly limiting the forward speed by the use of lower rotor-tip speeds at the maximum power output of the engine, inasmuch as the maximum forward speed is fixed by available power rather than by tip-stall considerations. For example, for the typical helicopter considered, in which advantage was taken of blade twist and an airfoil section having a high stalling angle, lowering the tip speed from 500 to 445 feet per second results in 8 percent less power required to hover at fixed weight. This reduction is equivalent to an increase of 5 percent in thrust at fixed power, or an increase of 27 percent in rate of vertical climb at fixed weight and power.

2. For a given limiting forward speed and with a single gear ratio, the incorporation of blade twist and the use of airfoil sections having high stalling angles increases the rotor vertical-flight performance by permitting the choice of a lower tip speed.

3. Further improvement in vertical-flight performance may be obtained by reducing the tip speed below the value at which tip stall in forward flight limits the maximum forward speed of the machine. The reduction in maximum forward speed due to tip stall, however, is extremely rapid when a single engine-to-rotor gear ratio is used.

4. When the rotor solidity is reduced, equivalent performance in both hovering and forward flight is obtained at higher tip speeds than those required by the higher-solidity rotor. The tip-speed requirements for the two flight conditions still conflict, however, inasmuch as the difference in tip speed required for optimum hovering performance and for a given limiting forward speed is similar for the two solidities.

5. For high-powered, cleanly designed machines, relatively high forward speeds and near-optimum vertical-flight performance can be obtained only through the use of a gear shift that enables full power to be drawn at

low tip speeds in vertical flight and at high tip speeds in maximum-forward-speed flight.

Langley Memorial Aeronautical Laboratory
National Advisory Committee for Aeronautics
Langley Field, Va.

APPENDIX

DERIVATION OF PERFORMANCE EQUATIONS FOR CONSTANT-CHORD, IDEALLY TWISTED BLADE IN VERTICAL-CLIMB CONDITION

From simple blade-element theory, the expression for the differential lift on a rotor-blade element operating at a distance r from the axis of rotation may be written as

$$dT = b\frac{1}{2}\rho(\Omega r)^2 c_l c \, dr \tag{A1}$$

Since

$$c_l = a_o \alpha_o$$

$$= a_o\left(\theta - \frac{u}{\Omega r}\right)$$

equation (A1) becomes

$$dT = \frac{b}{2}\rho\Omega^2 r^2 a_o\left(\theta - \frac{u}{\Omega r}\right)c \, dr \tag{A2}$$

The differential lift on the blade element may also be written from momentum considerations as

$$dT = 4\pi\rho u v r \, dr \tag{A3}$$

Equating expressions (A2) and (A3), letting $u = V_v + v$, and solving for v gives

$$v = \left(\frac{V_v}{2} + \frac{bca_o\Omega}{16\pi}\right)\left(-1 + \sqrt{1 + \frac{2\Omega r\left(\theta - \frac{V_v}{\Omega r}\right)}{\frac{4\pi V_v^2}{bca_o\Omega} + V_v + \frac{bca_o\Omega}{16\pi}}}\right) \tag{A4}$$

When the expressions for σ and x are substituted, equation (A4) becomes

$$v = \left(\frac{V_v}{2} + \frac{\sigma a_o \Omega R}{16}\right)\left(-1 + \sqrt{1 + \frac{2(x\theta\Omega R - V_v)}{\frac{4V_v^2}{\sigma a_o \Omega R} + V_v + \frac{\sigma a_o \Omega R}{16}}}\right) \quad (A5)$$

Since

$$\phi = \frac{V_v + v}{x\Omega R}$$

the general expression for the induced angle of attack of a blade element is

$$\phi = \left(\frac{V_v}{2x\Omega R} + \frac{\sigma a_o}{16x}\right)\left(-1 + \sqrt{1 + \frac{2(x\Omega R\theta - V_v)}{\frac{4V_v^2}{\sigma a_o \Omega R} + V_v + \frac{\sigma a_o \Omega R}{16}}}\right) + \frac{V_v}{\Omega R} \quad (A6)$$

The identical expression may be derived by means of vortex theory.

Equation (A5) shows that the downwash velocity may be made independent of the radial location of the blade element by setting $\theta = \frac{\theta_T}{x}$, where θ_T is the blade-tip pitch angle. This blade-angle distribution is known as the "ideal" twist, inasmuch as the induced-energy loss becomes a minimum with uniform downwash. For the case of ideal twist, equation (A6) then becomes

$$\phi_T = \phi x = \left(\frac{V_v}{2\Omega R} + \frac{\sigma a_o}{16}\right)\left(-1 + \sqrt{1 + \frac{2(\Omega R\theta_T - V_v)}{\frac{4V_v^2}{\sigma a_o \Omega R} + V_v + \frac{\sigma a_o \Omega R}{16}}}\right) + \frac{V_v}{\Omega R} \quad (A7)$$

The total thrust produced by the rotor may be written as

$$T = \int_0^{0.97} b\frac{\rho}{2}\Omega^2 R^3 a_o x(\theta_T - \phi_T)c\,dx \qquad (A8)$$

The upper limit of the integral is taken as $x = 0.97$ instead of $x = 1.0$ in order to take into account the loss of thrust at the rotor tip. As explained in the section entitled "Method of Analysis," this limit was chosen to make the procedure consistent with the forward-flight treatment of references 2 and 3. For the same reason, the limit of integration has been taken as $x = 1.0$ in deriving the torque expressions. Evaluating the integral in equation (A8) and equating it to the thrust expressed by

$$T = C_T \pi R^2 \rho (\Omega R)^2$$

yields

$$\frac{C_T}{0.941} = \frac{\sigma}{4} a_o (\theta_T - \phi_T) \qquad (A9)$$

where ϕ_T is given by equation (A7).

The induced plus potential-energy torque may be expressed as

$$Q_i + Q_{P.E.} = \int_0^1 b\frac{\rho}{2}\Omega^2 R^4 a_o x(\theta_T - \phi_T)\phi_T c\,dx \qquad (A10)$$

Equation (A10) gives an expression for induced-torque losses and the torque expended in changing the potential energy of the helicopter when climbing. Integrating the right-hand member of equation (A10) and equating it to the torque expressed by

$$Q_i + Q_{P.E.} = \left(C_{Q_i} + C_{Q_{P.E.}}\right)\pi R^2 \rho(\Omega R)^2 R$$

yields

$$C_{Q_i} + C_{Q_{P.E.}} = \frac{1}{4}\sigma a_o(\theta_T - \phi_T)\phi_T \qquad (A11)$$

In a similar way the profile-drag torque may be expressed as

$$Q_o = \int_0^1 b\frac{\rho}{2}\Omega^2 R^4 x^3 c c_{d_o}\, dx \qquad (A12)$$

If it is assumed that the section profile-drag coefficient is expressed by the function of a_o,

$$c_{d_o} = \delta_o + \delta_1 a_o + \delta_2 a_o^2$$

equation (A12) becomes

$$Q_o = b\frac{\rho}{2}\Omega^2 R^4 c \int_0^1 x^3\left[\delta_o + \frac{\delta_1}{x}(\theta_T - \phi_T) + \frac{\delta_2}{x^2}(\theta_T - \phi_T)^2\right] dx \qquad (A13)$$

Integrating the right-hand member of equation (A13) and equating it to the profile-drag torque expressed by

$$Q_o = C_{Q_o}\pi R^2 \rho(\Omega R)^2 R$$

yields

$$C_{Q_o} = \frac{\sigma}{2}\left[\frac{\delta_o}{4} + \frac{\delta_1}{3}(\theta_T - \phi_T) + \frac{\delta_2}{2}(\theta_T - \phi_T)^2\right] \qquad (A14)$$

The total torque absorbed by the rotor is the sum of the induced, potential-energy, and profile-drag torques and is equal to

$$C_Q = \frac{\sigma}{2}\left[\frac{a_o}{2}(\theta_T - \phi_T)\phi_T + \frac{\delta_o}{4} + \frac{\delta_1}{3}(\theta_T - \phi_T) + \frac{\delta_2}{2}(\theta_T - \phi_T)^2\right] \quad (A15)$$

If equations (A7) and (A9) are solved simultaneously,

$$\phi_T = \frac{1}{2}\sqrt{\left(\frac{V_v}{\Omega R}\right)^2 + 2\frac{C_T}{0.941}} + \frac{1}{2}\frac{V_v}{\Omega R} \quad (A16)$$

and

$$\theta_T = \frac{1}{2}\sqrt{\left(\frac{V_v}{\Omega R}\right)^2 + 2\frac{C_T}{0.941}} + \frac{4}{\sigma a_o}\frac{C_T}{0.941} + \frac{1}{2}\frac{V_v}{\Omega R} \quad (A17)$$

When equations (A16) and (A17) are substituted in equation (A15),

$$C_Q = \frac{1}{2}\frac{C_T}{0.941}\sqrt{\left(\frac{V_v}{\Omega R}\right)^2 + \frac{2C_T}{0.941}} + \frac{1}{2}\frac{V_v}{\Omega R}\frac{C_T}{0.941} + \frac{\sigma}{8}\delta_o + \frac{2}{3}\frac{\delta_1}{a_o}\frac{C_T}{0.941} + \frac{4\delta_2}{\sigma a_o^2}\left(\frac{C_T}{0.941}\right)^2 \quad (A18)$$

The vertical-climb performance of a rotor of particular solidity and section characteristics may be calculated at any operating thrust coefficient by equation (A18). Hovering performance is obtained by setting $V_v/\Omega R = 0$ in this equation.

The vertical-climb velocity at a fixed weight and power can also be obtained from equation (A18) as

$$V_v = \Omega R\left[\frac{0.941}{C_T}\left(C_Q - C_{Q_o}\right) - \frac{1}{2}\left(\frac{C_T}{0.941}\right)^2\frac{1}{C_Q - C_{Q_o}}\right] \quad (A19)$$

In the use of this equation C_Q is calculated from power available and C_{Q_o} is calculated from the last three terms of equation (A18).

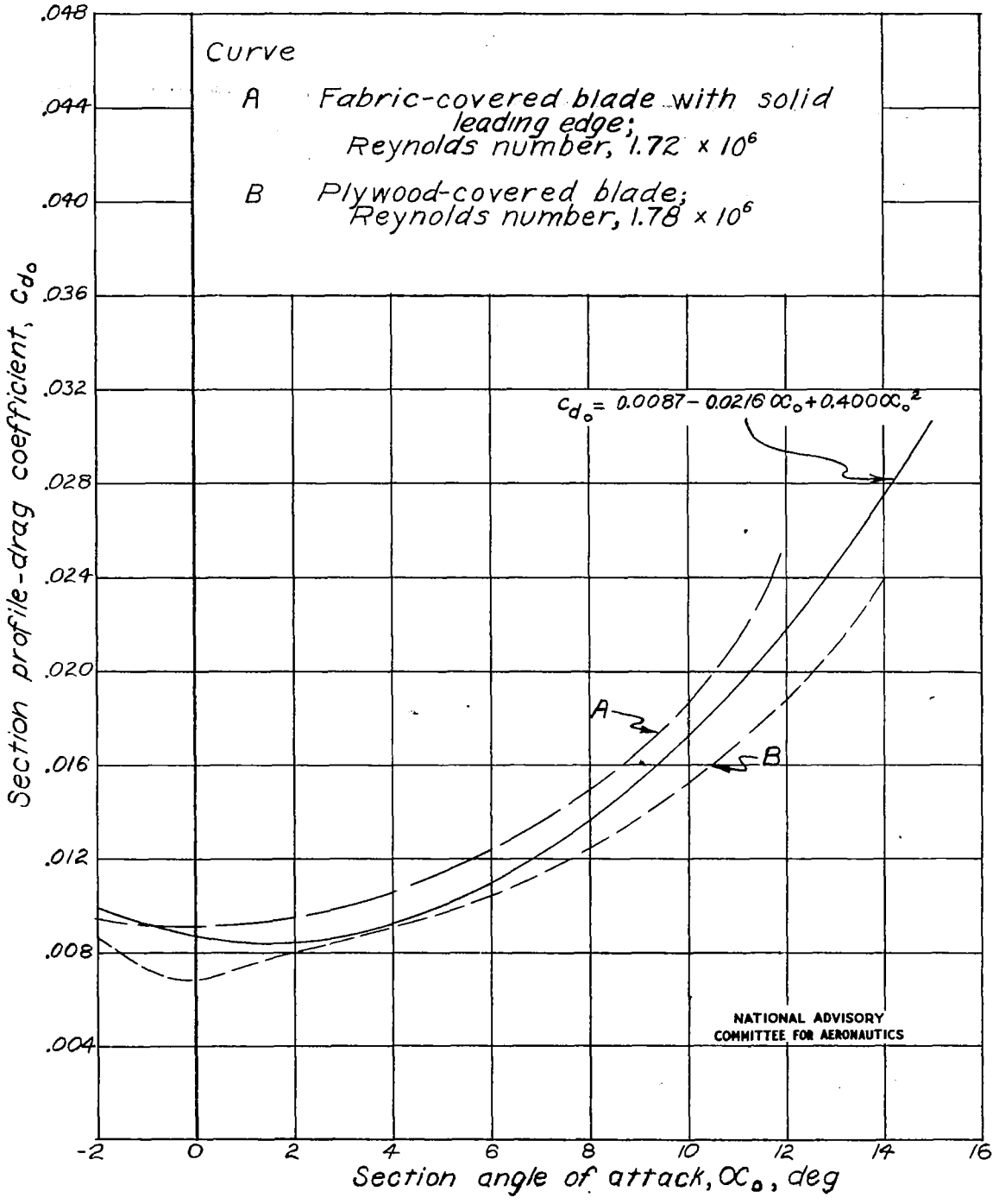

Figure 1.- Comparison of power-series profile-drag curve used in analysis with unpublished experimental data on practical-construction rotor-blade specimens having NACA 0012 section obtained in Langley two-dimensional low-turbulence pressure tunnel.

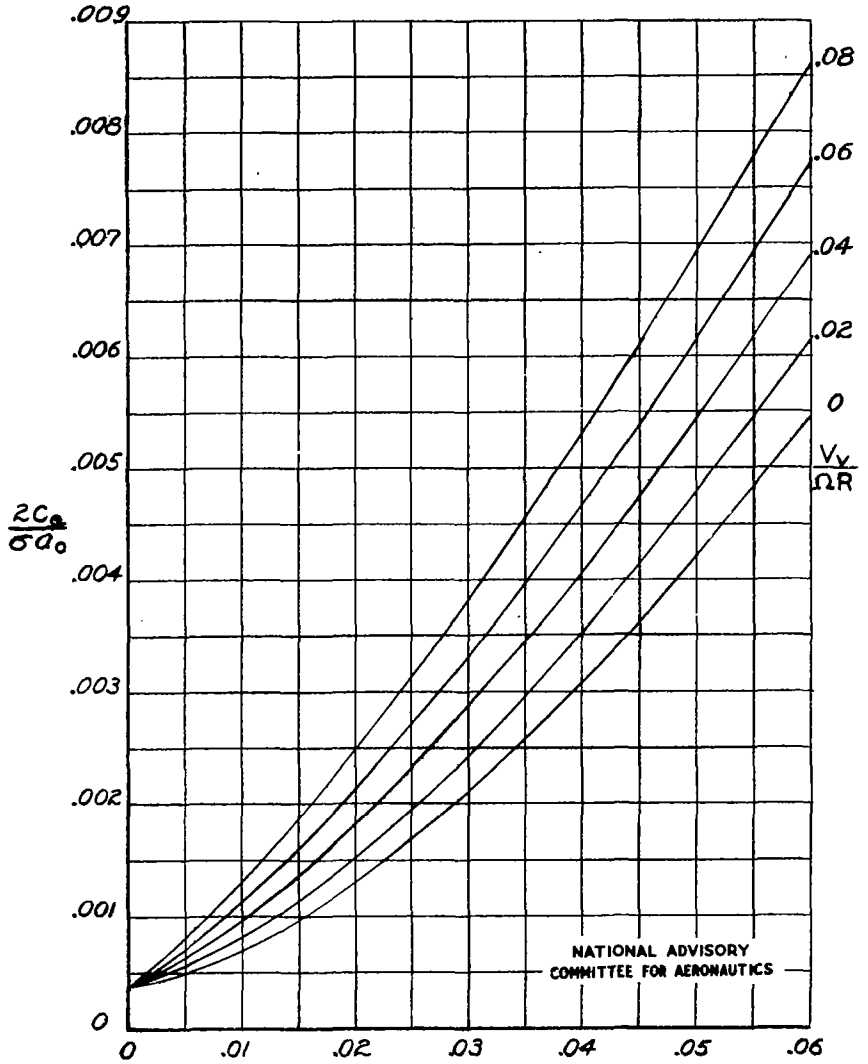

(a) $\sigma = 0.060$.

Figure 2. - Vertical-flight performance charts from theory based on the following assumptions: Uniform inflow distribution, $c_{d_0} = 0.0087 - 0.0216\alpha_0 + 0.400\alpha_0^2$, and $a_0 = 5.73$.

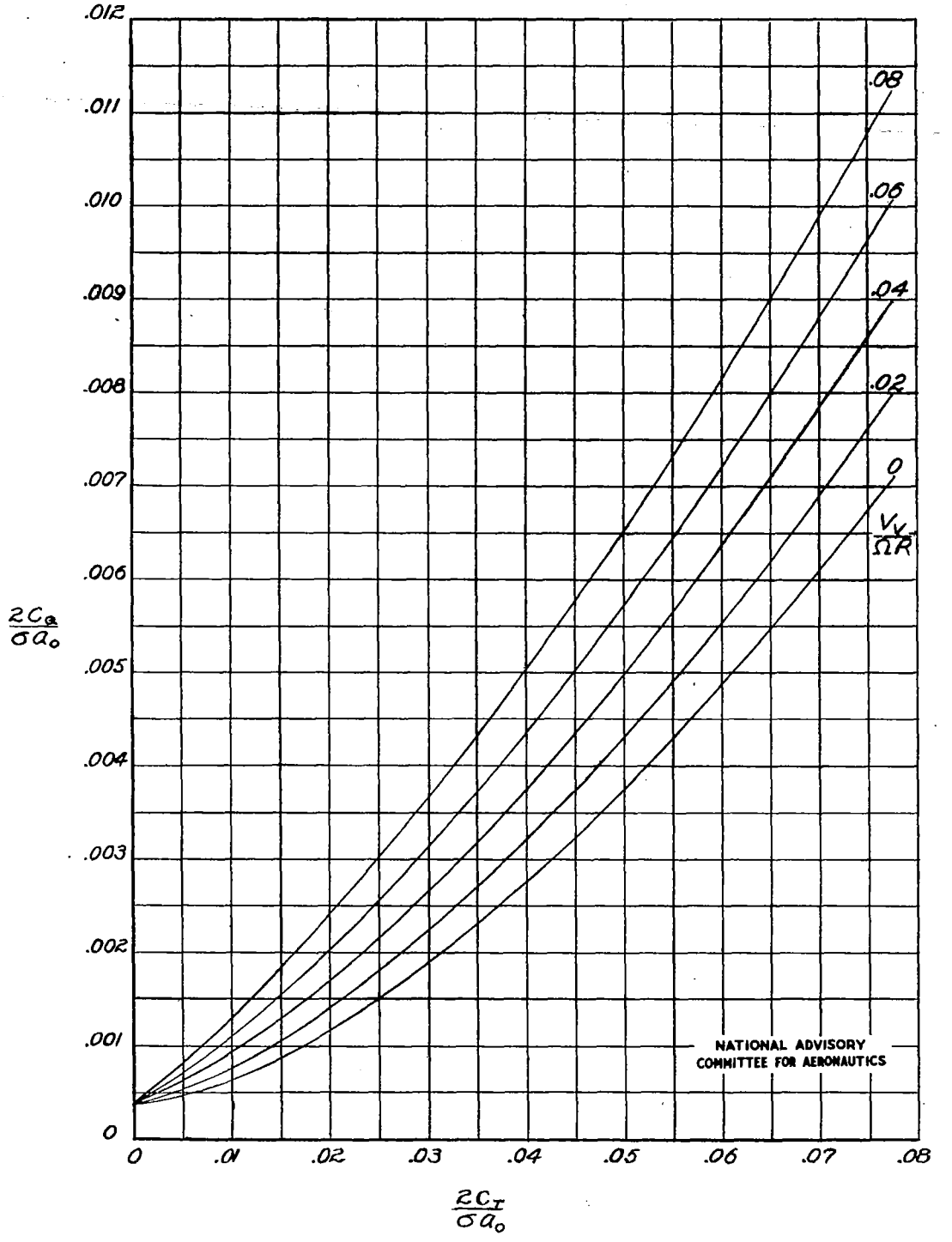

(b) $\sigma = 0.045$.

Figure 2. - Concluded.

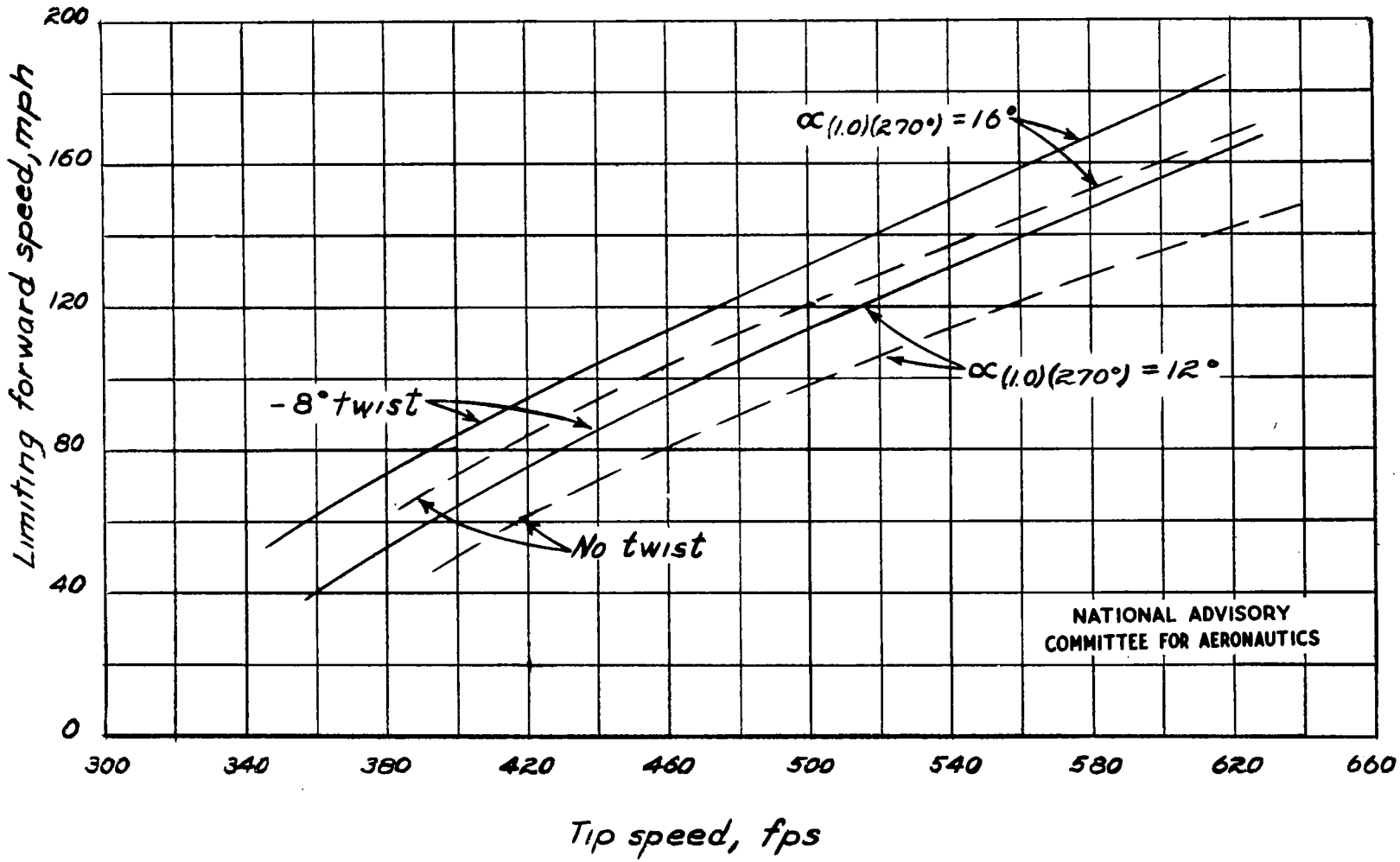

Figure 3.- Effect of blade twist and airfoil section on limiting forward speed of "typical" helicopter. W = 2700 pounds; $\bar{\sigma}$ = 0.060; R = 20.5 feet; altitude, 5000 feet.

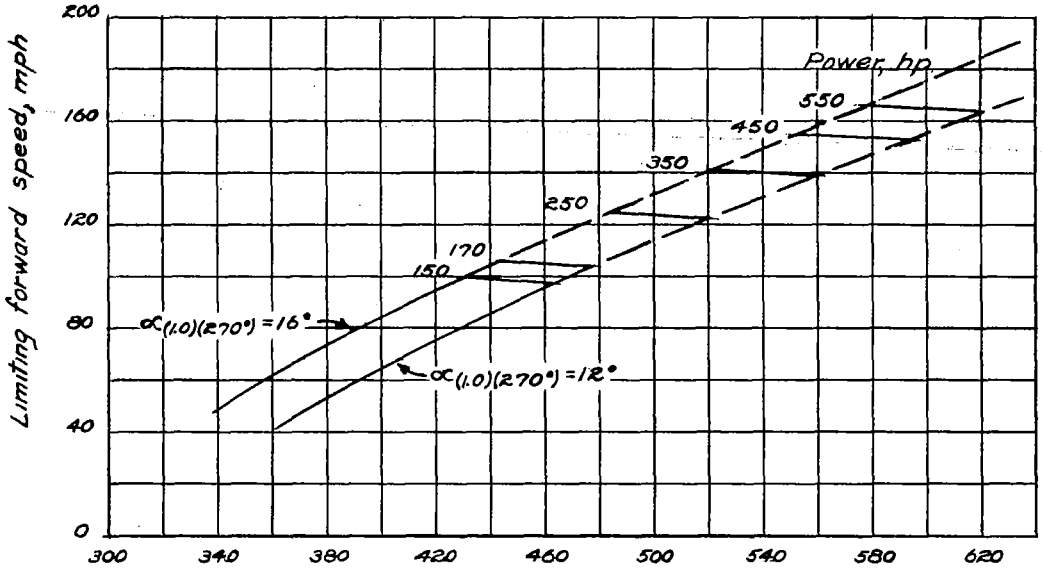

(a) Limiting forward speed and power required at altitude of 5000 feet.

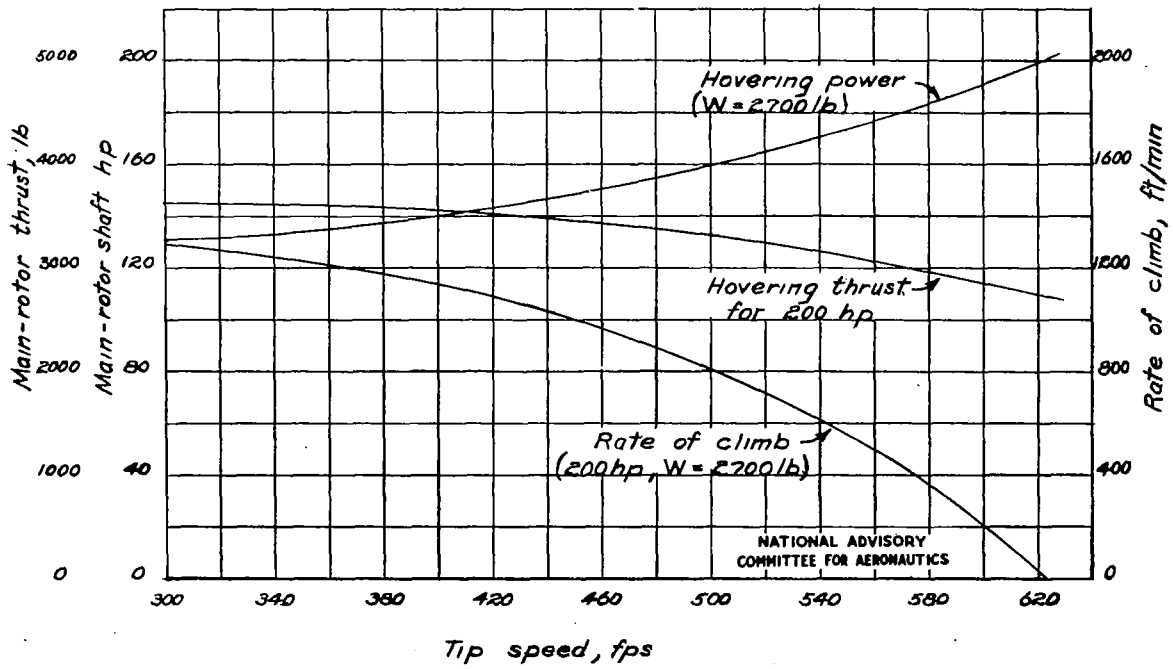

(b) Vertical-flight performance at sea level.

Figure 4.- Effect of tip speed on limiting forward speed and vertical-flight performance of "typical" helicopter. W = 2700 pounds; $\sigma = 0.060$; R = 20.5 feet.

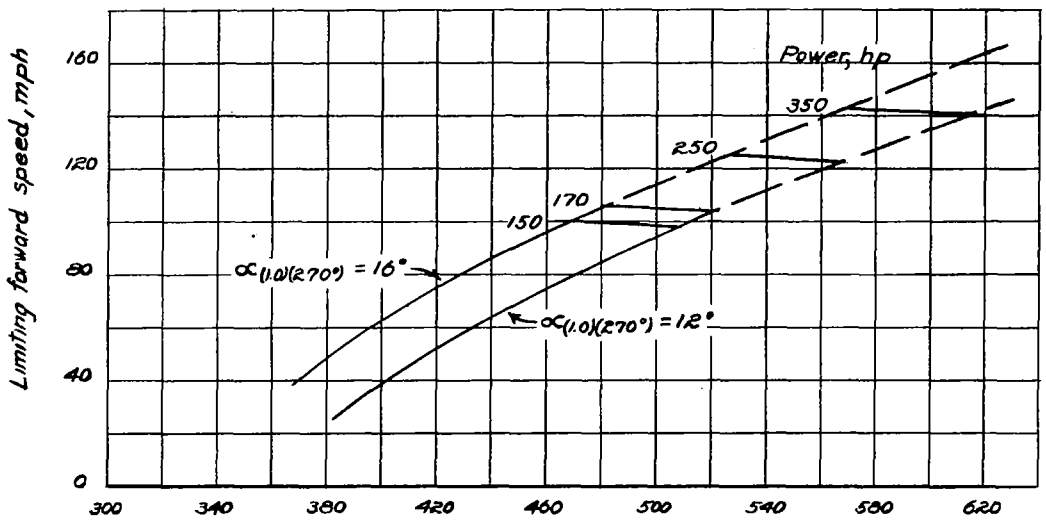

(a) Limiting forward speed and power required at altitude of 5000 feet.

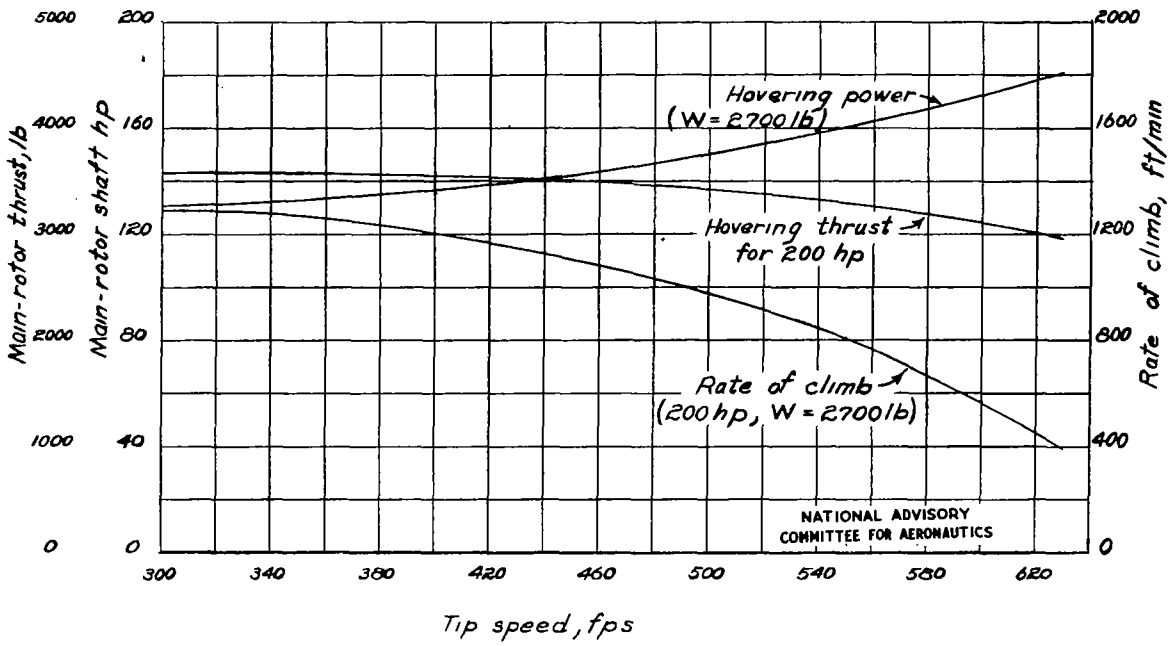

(b) Vertical-flight performance at sea level.

Figure 5.- Effect of tip speed on limiting forward speed and vertical-flight performance of "low-solidity" helicopter. W = 2700 pounds; σ = 0.045; R = 20.5 feet.

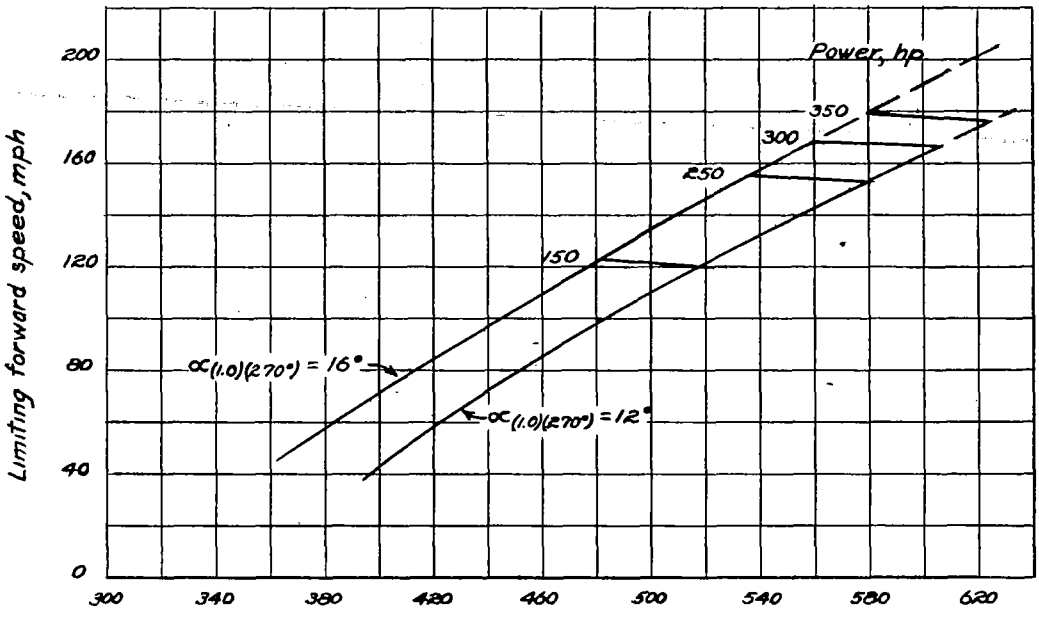

(a) Limiting forward speed and power required at altitude of 5000 feet.

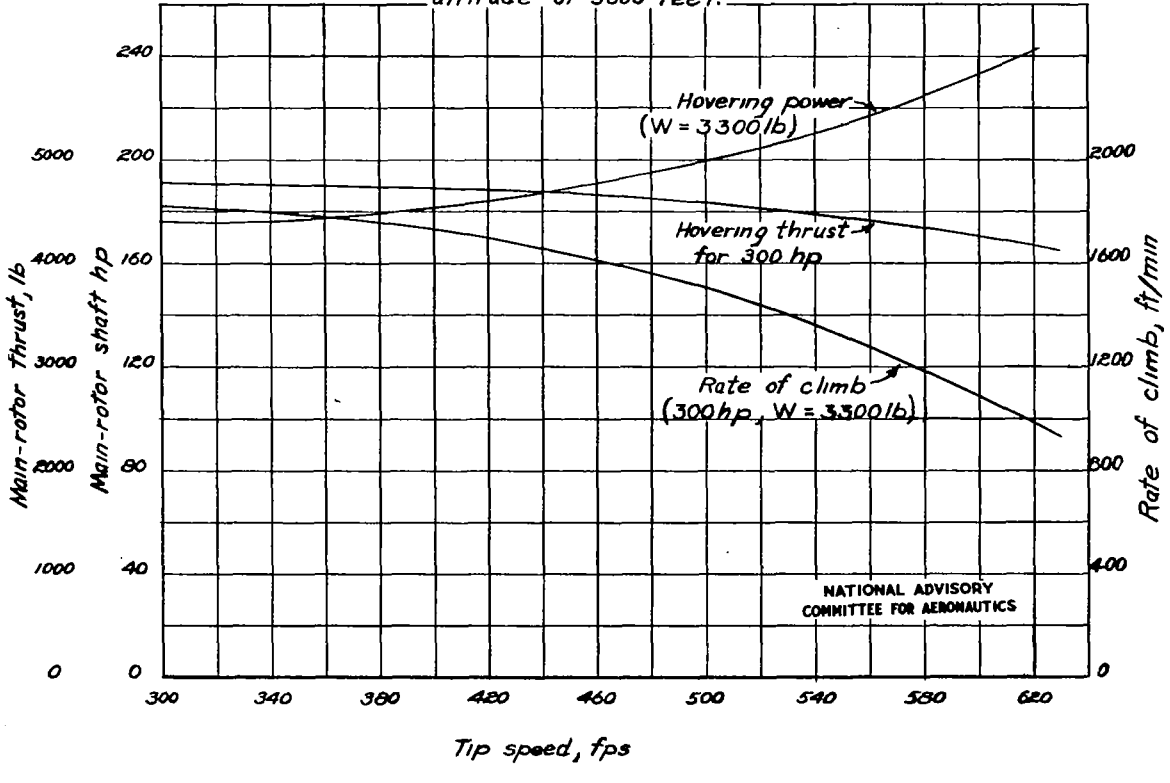

(b) Vertical-flight performance at sea level.

Figure 6.- Effect of tip speed on limiting forward speed and vertical-flight performance of "high-speed" helicopter. W = 3300 pounds; σ = 0.060; R = 20.5 feet.